Evaluation of Spanwise Variable Impedance Liners with Three-Dimensional Aeroacoustics Propagation Codes

M. G. Jones[*], W. R. Watson[†], D. M. Nark[‡], and N. H. Schiller[§]

NASA Langley Research Center, Hampton, VA 23681

Three perforate-over-honeycomb liner configurations, one uniform and two with spanwise variable impedance, are evaluated based on tests conducted in the NASA Grazing Flow Impedance Tube (GFIT) with a plane-wave source. Although the GFIT is only 2" wide, spanwise impedance variability clearly affects the measured acoustic pressure field, such that three-dimensional (3D) propagation codes are required to properly predict this acoustic pressure field. Three 3D propagation codes (CHE3D, COMSOL, and CDL) are used to predict the sound pressure level and phase at eighty-seven microphones flush-mounted in the GFIT (distributed along all four walls). The CHE3D and COMSOL codes compare favorably with the measured data, regardless of whether an exit acoustic pressure or anechoic boundary condition is employed. Except for those frequencies where the attenuation is large, the CDL code also provides acceptable estimates of the measured acoustic pressure profile. The CHE3D and COMSOL predictions diverge slightly from the measured data for frequencies away from resonance, where the attenuation is noticeably reduced, particularly when an exit acoustic pressure boundary condition is used. For these conditions, the CDL code actually provides slightly more favorable comparison with the measured data. Overall, the comparisons of predicted and measured data suggest that any of these codes can be used to understand data trends associated with spanwise variable-impedance liners.

I.   Introduction

Acoustic liners have been employed for the reduction of aircraft fan noise for approximately six decades. In the early years, these liners consisted of single-degree-of-freedom (SDOF), single-layer structures (see Fig. 1a) tuned to absorb selected tones (e.g., multiples of the blade passage frequency). As the bypass ratio of commercial aircraft engines increased, the dominant fan noise transitioned from tones to a combination of tones and broadband noise. This led to the introduction of double-degree-of-freedom (DDOF), two-layer liners (see Fig. 1b), which provided a significant increase in the noise reduction frequency range. A second approach was to use different SDOF liners in the inner and outer walls of the aft fan duct. In this latter approach, the inner and outer wall liners are tuned to different frequencies, and thus can be combined to achieve noise reduction over a wider frequency range.

Most modern aircraft employ one or both of these liner types in the inlet and aft-bypass duct. Conventional design practice typically assumes these SDOF and DDOF acoustic liners are uniform, i.e., each chamber within the liner is intended to be virtually identical to every other chamber within the liner. The usage of uniform liners enables efficient fabrication and simplifies the modeling process, such that the noise reduction can be reliably predicted.

The current trend in aircraft nacelle design is to further increase the bypass ratio, thereby decreasing the space allocated for acoustic liners. This trend is motivated by the need to further reduce the weight and drag due to acoustic liners, and to thereby reduce the amount of fuel required. Thus, there is increased

---

[*]Senior Research Scientist, Research Directorate, Structural Acoustics Branch, AIAA Associate Fellow.
[†]Senior Research Scientist, Research Directorate, Computational AeroSciences Branch, AIAA Associate Fellow.
[‡]Senior Research Scientist, Research Directorate, Structural Acoustics Branch, AIAA Associate Fellow.
[§]Research Scientist, Research Directorate, Structural Acoustics Branch.

American Institute of Aeronautics and Astronautics

interest in variable-impedance liner concepts, which offer the potential for (1) an extension of the frequency range over which noise reduction occurs, and (2) an increase in the amount of noise reduction achieved.
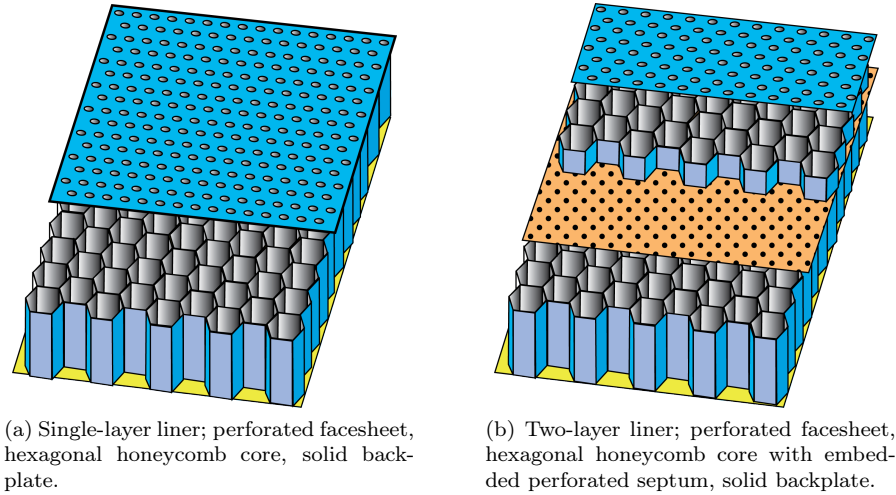

(a) Single-layer liner; perforated facesheet, hexagonal honeycomb core, solid backplate.

(b) Two-layer liner; perforated facesheet, hexagonal honeycomb core with embedded perforated septum, solid backplate.

Figure 1: Sketches of single- and double-degree-of-freedom (SDOF and DDOF) conventional liners.

Two distinct variable-impedance liner concepts have been considered. The first employs groups of liner chambers, each of which is designed to target a different frequency.[1,2] These groups of liner chambers are clustered within a small spatial extent, such that the resultant surface impedance of the liner can be properly modeled as uniform (sometimes labeled 'smeared impedance'). This concept offers the potential for increased broadband noise reduction,[3] but also adds complexity for the fabrication process. The second concept employs chambers of variable depth in the axial and/or circumferential directions. This concept is currently present in the aft duct of many aircraft due to the limited volume within the engine nacelle walls. Support hardware (e.g., wiring, air-conditioning ductwork) often infringes on the space available for installation of the acoustic liners, with the unintended consequence that the liner depth varies in the axial and/or circumferential directions.[4-7] One implementation of this latter concept is the axially-segmented liner, sometimes referred to as the zone liner. For this type of liner, each axial segment is designed such that the total effect is to achieve improved broadband absorption. For example, one axial segment may be used to scatter energy from a low-order mode in one axial segment to a higher-order mode in a subsequent axial segment, such that the subsequent axial segment can provide more effective sound absorption.

For those configurations where the impedance varies only in the axial dimension, a two-dimensional acoustic propagation code can be used to predict the effects of the liner on the acoustic wave as it propagates down the duct. If the impedance is allowed to vary in the spanwise dimension, multiple scenarios are possible. Based on the results of a recent study,[8] if the spatial extent over which the impedance is allowed to vary is less than one-third of a wavelength for the frequency of interest, then the liner can be properly modeled as a uniform (smeared) impedance. Under these circumstances, it is appropriate to continue to use a 2D propagation code to model the aeroacoustic field throughout the duct. As the frequency increases, this criteria becomes increasingly more difficult to satisfy. Also, the possibility exists for energy to transfer from one soft-wall mode to another. For either of these cases, three-dimensional propagation codes are needed.

This was made evident in a recent ONERA-NASA collaboration,[9] in which impedances educed in the ONERA B2A wind tunnel were compared with those obtained using the NASA Langley Grazing Flow Impedance Tube (GFIT). Tests were conducted in each flow duct with similar liners. The comparisons were acceptable, but there were sufficient differences to warrant further analysis. One cause of the discrepancies is believed to be the difference in the facesheets used for the two liners. The treated portion (that portion of the liner facesheet that contains perforations) extended across the full 2.0" width of the NASA GFIT, but only extended across the centered span (1.2" of the total 2.0" width) of the ONERA B2A duct. This latter choice was due to the usage of Laser Doppler Anemometry to measure the acoustic particle velocity at the

American Institute of Aeronautics and Astronautics

surface of the treated portion of the liner. Given the small spanwise dimension of the B2A (2.0"), it seemed reasonable to assume that the surface impedance of the liner could be treated as uniform (smeared) over the width of the duct, albeit with a reduced effective porosity. Indeed, some of the differences between the NASA and ONERA results could be explained by this assumption, but it became evident that there were also three-dimensional effects present.

The purpose of the current study is to more thoroughly explore the effects of spanwise variable impedance in a controlled aeroacoustic environment. Specifically, three liner configurations are evaluated based on tests conducted in the NASA GFIT with a plane-wave source. The first configuration is a conventional perforate-over-honeycomb liner, with uniform impedance over the full width of the duct. The other two liner configurations employ multiple spanwise segments, where one of the segments in each liner configuration employs the same structure (perforate-over-honeycomb) as was used for the uniform impedance liner and the remaining spanwise segments are solid (i.e., the active portion of liner does not extend across the full width of the duct).

Three 3D acoustic propagation codes are used to compare with the data measured in the GFIT. These include the CHE3D,[10] CDL,[11] and COMSOL.[12] The first two codes are NASA codes, while the last is commercially available. These codes employ distinct approaches to model the aeroacoustic environment within the GFIT. Thus, the primary goal of the current investigation is to explore the validity of each code for use in the design and evaluation of spanwise variable impedance liners.

In the current study, each of the three liner configurations mentioned above (one uniform and two spanwise variable impedance liner configurations) is tested in the NASA GFIT with a 140 dB, single-tone source (frequencies from 400 to 3000 Hz), at grazing flow Mach numbers of 0.0 and 0.3. First, the measured acoustic pressures are used to directly assess the effects of varying the impedance in the spanwise dimension. Acoustic pressure data acquired with the uniform liner is then used with the Kumaresan and Tufts (KT) method[13] to educe the acoustic impedance, which is assumed to be the same for the treated portion of each of the three liner configurations (the treated portion for each liner is identical). This impedance is used as an input to each of the 3D propagation codes (assuming a plane-wave source), and each code is used to predict the acoustic pressures at each of the eighty-seven microphone locations in the GFIT. These microphone locations are distributed among all four walls (fore and aft of the liner in the upper wall, and throughout the test section in the other three walls). The comparison is used to assess the ability of each of these propagation codes to account for spanwise impedance variability.

Section II provides a description of the Grazing Flow Impedance Tube and the three liner configurations considered in this study. Section III provides a description of the impedance eduction method. The acoustic propagation models are briefly described in Section IV, and results are provided in Section V. Finally, concluding remarks are provided in Section VI.

II. Experimental Method

A. Grazing Flow Impedance Tube

All liners considered in this study are designed to fit in the GFIT. The GFIT (see Fig. 2) has a cross-sectional geometry of 2.0"-wide by 2.5"-high, and allows evaluation of acoustic liners with lengths from 2.0" to 24.0". The surface of the test liner forms a portion of the upper wall of the flow duct. Twelve acoustic drivers form an upstream (exhaust mode) source section. For this study, these drivers are used to generate tones (one frequency at a time) over a frequency range of 400 to 3000 Hz, at source levels (measured at the reference microphone) of 140 dB, and at centerline Mach numbers of 0.0 and 0.3. Eighty-seven (87) microphones are flush-mounted in the four walls of the GFIT, and are used to measure the acoustic pressure field over the spatial extent of $\{0 \leq x \leq L, 0 \leq y \leq H, 0 \leq z \leq W\}$, where L, H, and W represent the length (40.0"), height (2.5"), and width (2.0"), respectively, of the test section.

B. Liner Configurations

Three 2.0"-wide by 16.0"-long liner configurations, labeled as SVC1, SVC2, and SVC3, are evaluated in this study (see Fig. 3). Each liner consists of a 4×30 array of square (0.4"×0.4") chambers separated by 0.135"-

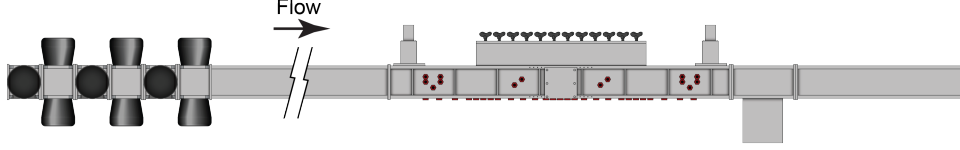American Institute of Aeronautics and Astronautics

Figure 2: Sketch of Grazing Flow Impedance Tube (GFIT).

wide axial partitions and 0.13"-wide spanwise partitions. The SVC1 liner is uniform (i.e., every chamber is identical), but the SVC2 and SVC3 liners are nonuniform. For the SVC2 liner, two adjacent axial rows of chambers are solid and the other two employ the same design as is used for the SVC1 liner. For the SVC3 liner, the two treated rows are centered (spanwise), and the rows of solid chambers are at the left and right edges. The SVC1 and SVC3 liners are symmetric, such that the orientation should not affect the measured acoustic pressure distribution throughout the GFIT. This is not true for the SVC2 liner. Thus, it should be noted that the SVC2 liner was tested with the two treated rows of chambers on the left facing downstream.

The treated portions of each of these liners are identical. Each treated chamber consists of an 0.034"-thick perforated facesheet that contains 22 holes with a diameter of 0.041". This results in an overall porosity (including the effects of the partitions) of 11%. The core depth of each chamber is 3.0".
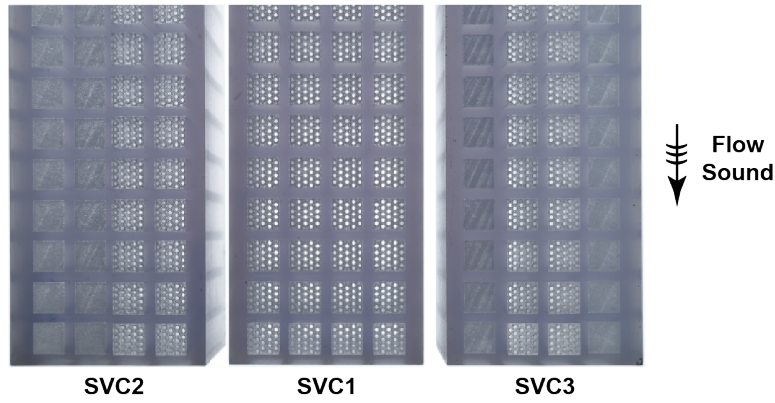
Figure 3: Close-up photograph of SVC1 (uniform impedance), SVC2 (asymmetric variable impedance), and SVC3 (symmetric variable impedance) liners. Top View.

III.   Impedance Eduction

The Kumaersan and Tufts (KT) method is used to educe the impedance of the uniform liner (SVC1). This method is described in detail in an earlier paper.[10] Therefore, only enough detail is presented to motivate the methods and goals of the current investigation. First, the acoustic pressures (sound pressure level, SPL, and phase, ϕ) are measured with twelve evenly-spaced microphones (each 1" apart) mounted on the wall opposite the liner. These data are then used to expand the acoustic pressure field in the liner test section into a series of normal duct modes. Associated with each normal mode is an unknown axial propagation constant that is measured via the microphone data and the KT method. Each normal mode satisfies the convected Helmholtz equation and the lower wall boundary condition. This normal mode solution (with the axial propagation constant determined using the KT method) is then substituted into the wall impedance boundary condition to give an exact expression for the impedance. Since the treated portions (i.e., the portions that contain a perforated facesheet) of all three test liners are designed to be identical, it is assumed that their impedances are also identical. These impedances are used as input for the propagation codes (see Sec. IV), such that the SPL and phase can be predicted at each microphone location in the GFIT.

American Institute of Aeronautics and Astronautics

IV. Duct Acoustic Propagation Codes

Three 3D duct acoustic propagation codes (CHE3D,[10] CDL,[11] and COMSOL[12]) are used in this study. These codes are described in detail in the cited references, so only those details that are key to the current study are provided herein. Each of these codes solves the convected Helmholtz equation and, for the purposes of this study, employs a uniform flow profile and a plane-wave source. They also assume the liner to be installed on the upper wall, as in the GFIT, and allow the impedance to be specified over the surface of the liner.

Both CHE3D and COMSOL solve a second order partial differential equation using a conventional Galerkin finite element method. These codes include the effects of reflections at the leading and trailing edges of the liner and have the potential to capture reflections at the duct termination. CHE3D uses the acoustic pressure variable as the unknown, whereas COMSOL uses the acoustic potential as the unknown variable. Further, COMSOL uses cubic Lagrange shape functions in which the acoustic potential is the only unknown at grid points (and internal nodes), while CHE3D uses cubic Hermite shape functions in which the acoustic pressure and its derivatives are unknowns at the grid points. For the current study, each of these codes is implemented with two termination boundary conditions. A ρc termination is assumed (anechoic if the sound field consists solely of plane waves in the untreated duct section downstream of the liner trailing edge) for the first set of computations (labeled as CHE,ρc and COM,ρc), and an acoustic pressure boundary condition is assumed for the second set of computations (labeled as CHE,P and COM,P). This acoustic pressure is set to match the acoustic pressure measured via one of the microphones mounted in the termination plane.

The CDL propagation code utilizes a parabolic approximation to the convected Helmholtz equation with the acoustic potential as the unknown variable. The CDL is a computationally efficient model that is generally of lower fidelity than the CHE and COMSOL models, since it neglects reflections due to impedance discontinuities at the leading and trailing edges of the liner. It also assumes the duct termination is anechoic.

V. Results and Discussion

The results are separated into three categories. First, a direct comparison of the measured sound pressure level profiles, SPL(x), is used to compare the effects of the three liner configurations. These results are used to determine the need for 3D propagation codes to evaluate the effects of spanwise impedance variability for GFIT samples. Next, the KT method is used to educe the impedance of the uniform liner (SVC1). The treated portions of the other two liners (SVC2 and SVC3) are identical to the SVC1 liner. Thus, this same impedance spectrum is used as an input for the 3D propagation codes for the treated portions of each liner. The untreated portions of the SVC2 and SVC3 liners are assumed to be acoustically rigid (hard wall). The third set of results provides a comparison of predicted and measured SPLs at each microphone location.

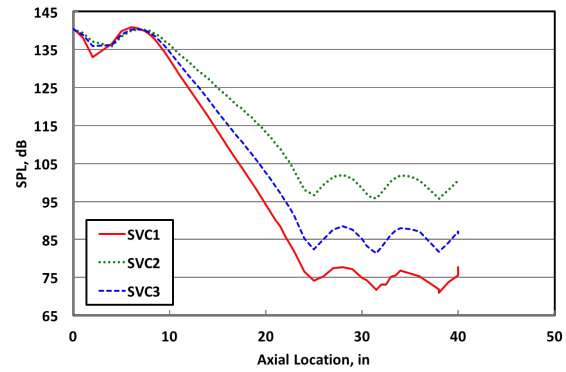## A. Measured Sound Pressure Levels

Figures 4 and 5 provide a comparison of measured SPLs at each of the microphone locations along the lower wall (57 microphones mounted on the wall opposite the liner) in the GFIT, for frequencies of 600 to 2200 Hz in 400 Hz increments. Although these microphones are distributed across the span of the lower wall, they are treated as if they are in a straight line for plotting purposes. If the zero-order mode in the spanwise dimension is dominant, each of the measurements is representative of what would be measured at any position across the span of the lower wall. However, for those configurations where the impedance varies across the span of the duct, the likelihood of higher-order mode content increases. Since the spanwise modal content is not known *a priori*, it is important to keep in mind the potential effects of spanwise variability. These measurements are connected by solid lines for ease of display. Results for the SVC1 (uniform), SVC2 (asymmetric variable impedance), and SVC3 (symmetric variable impedance) liner configurations are depicted with solid red, dotted green, and dashed blue lines, respectively.

A few items are readily apparent in these figures. Each of the liners provides excellent sound absorption at 1000 Hz. The absorption is much greater at Mach 0.0, but remains significant at Mach 0.3. There is minimal attenuation at Mach 0.0 for the remainder of the frequency range. This improves at Mach 0.3, where the attenuation is evident for the frequencies just below (600 Hz) and above (1400 Hz) 1000 Hz. This
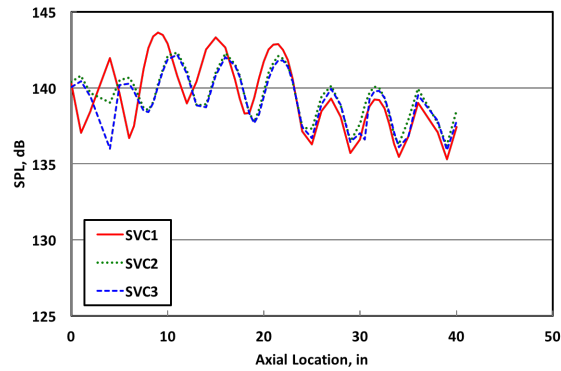
is to be expected for this type of SDOF liner. Also, the evidence of standing waves is strong, indicating that the termination is non-anechoic. Finally, the measured SPLs are observed to be quite similar for the two spanwise variable impedance liners (SVC2 and SVC3) at most frequencies.
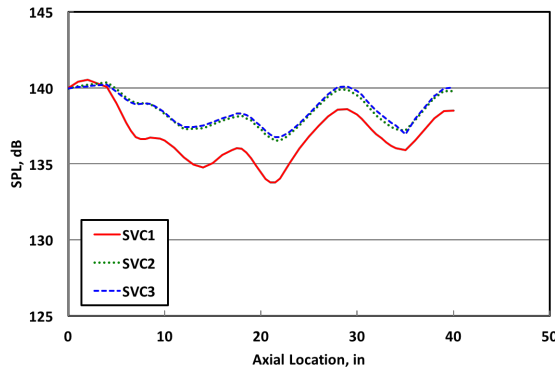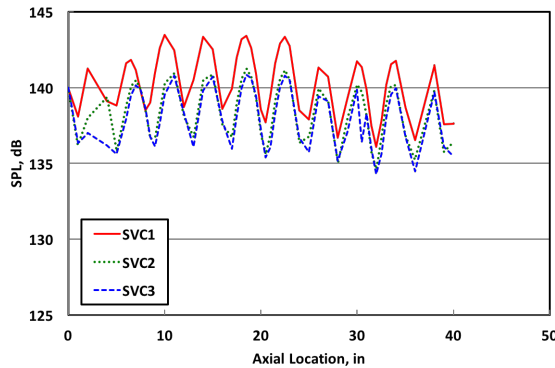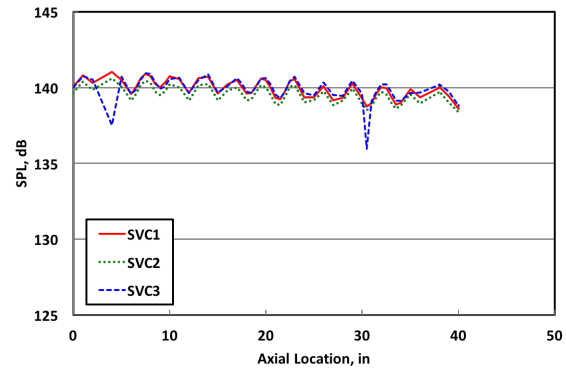

(a) 600 Hz source.

(b) 1000 Hz source.
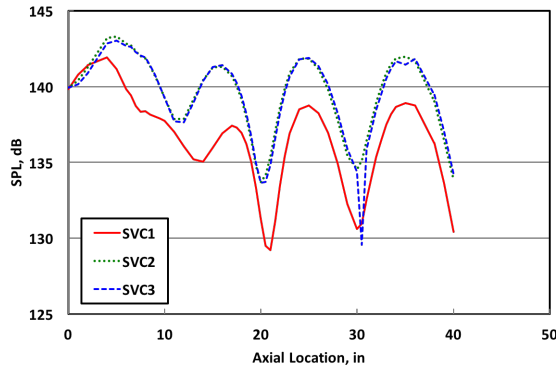

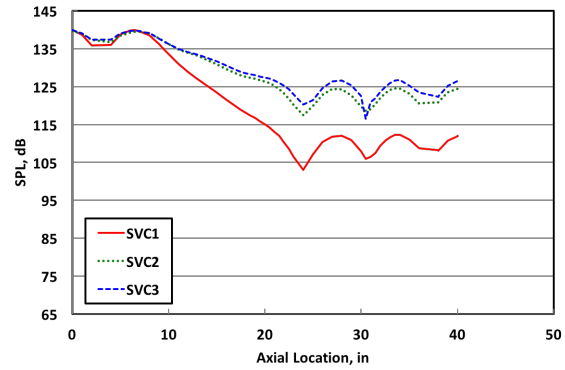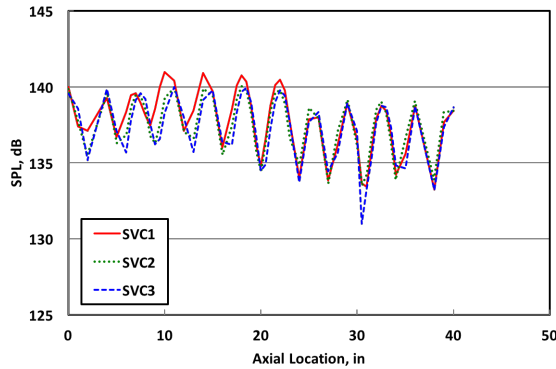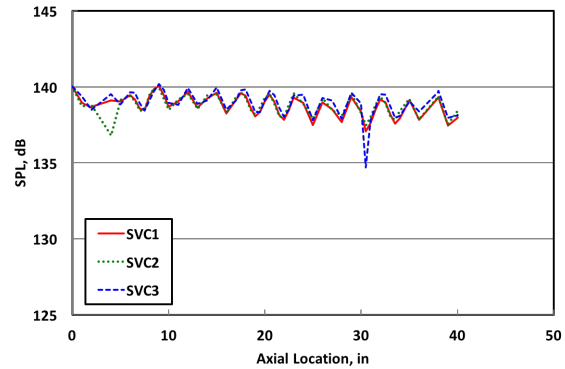(c) 1400 Hz source.

(d) 1800 Hz source.

(e) 2200 Hz source.

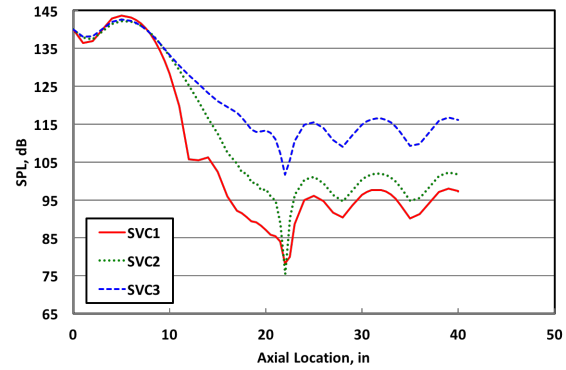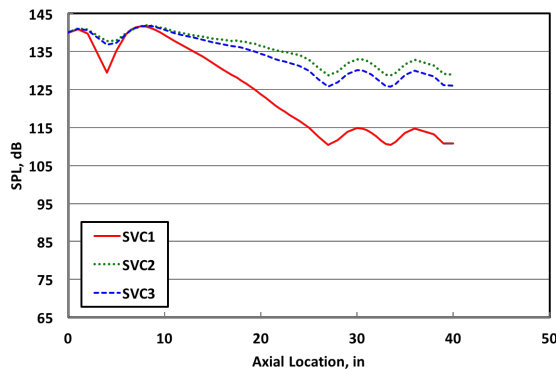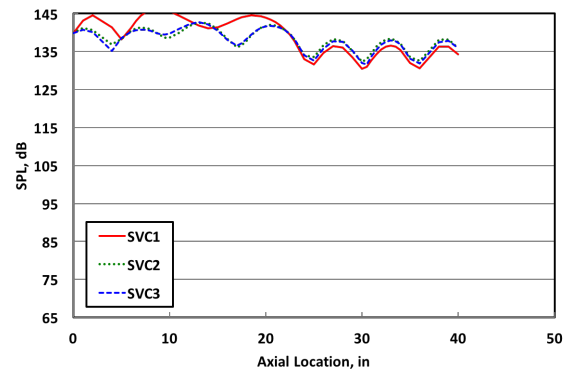Figure 4: Sound pressure level axial profile. Mach 0.0.

For a number of test conditions, the SVC2 and SVC3 results are very well matched, suggesting that a 2D analysis should be sufficient. However, the results for the SVC3 liner deviate from those of the SVC2 liner for some of the test conditions. This is particularly evident at 1000 Hz, where the liners provide significant

American Institute of Aeronautics and Astronautics

sound absorption. Although both of the variable-impedance liners (SVC2 and SVC3) contain an identical number of treated chambers, the respective SPL distributions are very different.

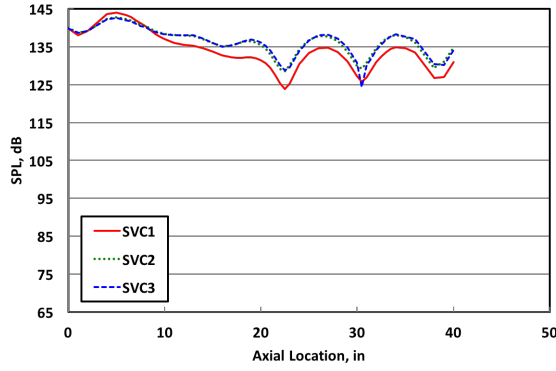(a) 600 Hz source.

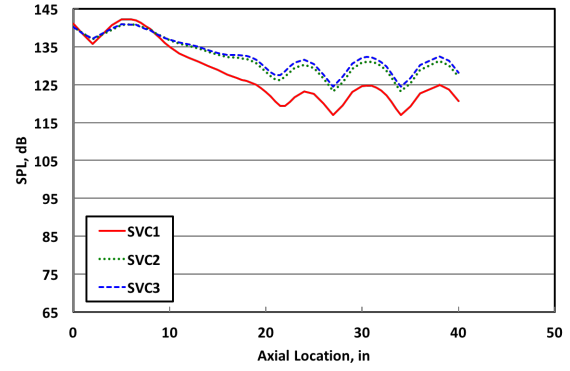(b) 1000 Hz source.
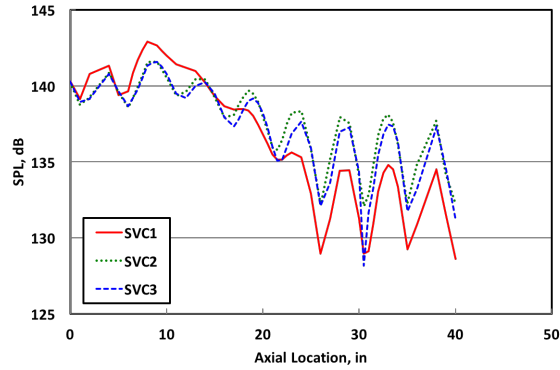
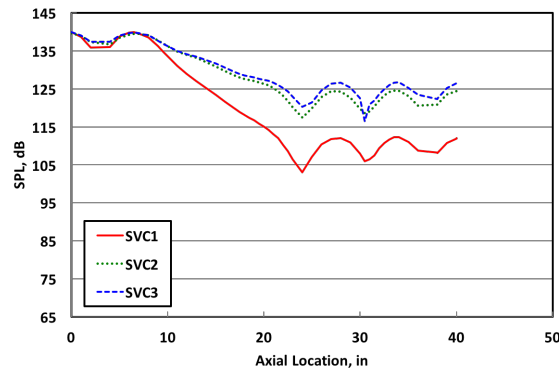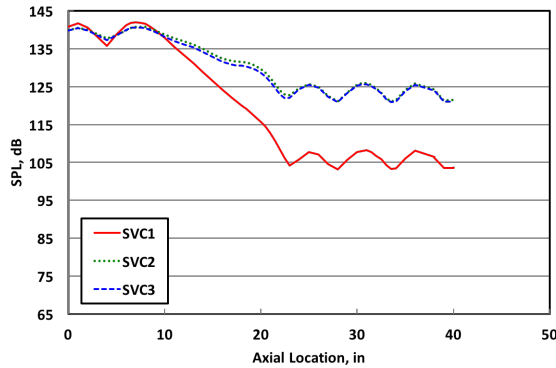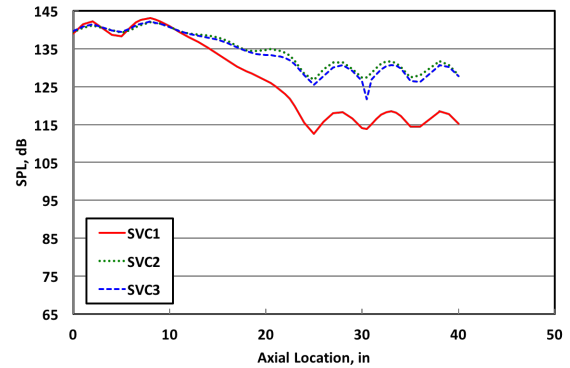(c) 1400 Hz source.

(d) 1800 Hz source.

(e) 2200 Hz source.

Figure 5: Sound pressure level axial profile. Mach 0.3.

An additional set of measurements was acquired to investigate the SPL profiles for frequencies near 1000 Hz. Specifically, data were acquired at frequencies of 800 to 1200 Hz in 50 Hz increments. A portion of these results is provided in figures 6 and 7. Overall, the results for the two spanwise variable-impedance liners (SVC2 and SVC3) are shown to be very similar when the total attenuation is minimal. However,

American Institute of Aeronautics and Astronautics

the SPL profiles for these two liners clearly diverge as the attenuation increases. This divergence of SPL profiles is present in the Mach 0.3 results, but is more evident at Mach 0.0 because these liners are tuned (via the facesheet geometry) for maximum attenuation at the no-flow condition. For those cases where this divergence occurs, it is a clear indication of the three-dimensional effects of the spanwise distribution of the treated chambers, i.e., a 3D analysis is required.
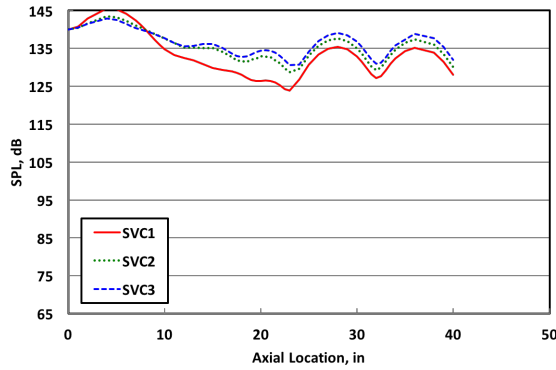
(a) 800 Hz source.

(b) 900 Hz source.
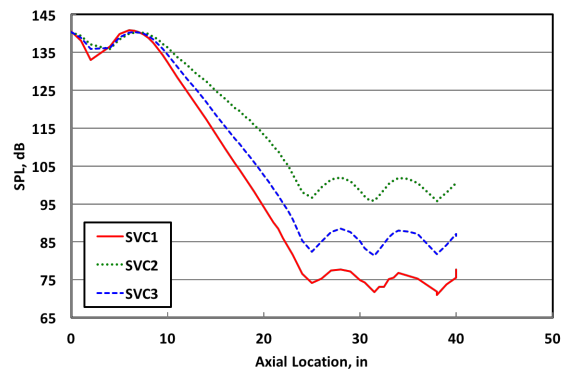
(c) 1000 Hz source.

(d) 1100 Hz source.

(e) 1200 Hz source.

Figure 6: Sound pressure level axial profile. Mach 0.0; Fine Resolution.

American Institute of Aeronautics and Astronautics

(a) 800 Hz source.

(b) 900 Hz source.

(c) 1000 Hz source.

(d) 1100 Hz source.

(e) 1200 Hz source.

Figure 7: Sound pressure level axial profile. Mach 0.3; Fine Resolution.

B. Educed Impedance Spectra

As indicated in Section III, the KT method was used to educe the impedance for the uniform liner (SVC1). Figure 8 provides a comparison of the normalized acoustic resistance and reactance spectra (all impedances are normalized by the quantity ρc, where ρ and c represent the density and sound speed in air, respectively) educed with the SVC1 liner mounted in the GFIT. The results are provided at 200 Hz increments across the full frequency range, and at 50 Hz increments for frequencies surrounding 1000 Hz, the frequency of

American Institute of Aeronautics and Astronautics

peak attenuation. As expected for this type of liner, the normalized resistance is observed to increase by approximately 0.5 at frequencies away from antiresonance (near 2200 Hz in this case) when the flow is on. With the exception of a few points at frequencies very near antiresonance, the normalized reactance is virtually unaffected by the change in Mach number from 0.0 to 0.3. Resonance occurs at a frequency between 1000 and 1200 Hz for both flow conditions. This explains the significant attenuation measured at 1000 Hz for each of the three liners. Finally, minimal attenuation should be expected in the vicinity of antiresonance (at or near 2200 Hz). These impedance spectra are assumed to be correct for the treated portions of the SVC2 and SVC3 liner configurations, as those liner portions are designed to be identical to the SVC1 liner.

(a) Acoustic resistance spectra. (b) Acoustic reactance spectra.
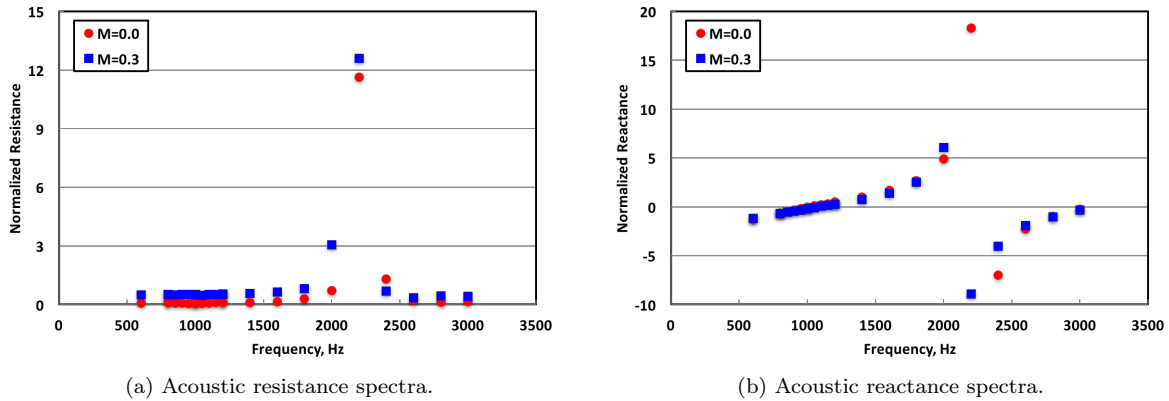
Figure 8: Normalized impedance spectra educed from the SVC1 acoustic pressure data using the KT method.

C. Comparison of Predicted and Measured Sound Pressure Levels

Figures 9 - 11 provide comparisons of predicted and measured SPLs for each of the three liners at two flow conditions (Mach 0.0 and 0.3), at frequencies of 1000, 1050, and 1100 Hz. These results were chosen for display because they demonstrate how the predictions compare with the measured data when the frequency diverges from 1000 Hz and the attenuation decreases. Each plot contains six curves. The measured data are depicted with 'x' symbols, and the predicted data are depicted with lines. Solid lines are used for the two codes that employ the exit pressure boundary condition, and dashed lines are used for the three codes that assume an anechoic termination. For each of the predictions, the measured SPL and phase in the source plane ($x = 0.0$", 8" upstream of the leading edge of the liner) are specified as an input boundary condition.

Overall, the CHE3D and COMSOL codes with exit pressure boundary conditions compare very favorably with the measured data. Those two predictions are virtually identical for the Mach 0.0 condition, and are very similar for the Mach 0.3 condition. When the termination is switched to anechoic, the comparison with measured data degrades slightly, but still remains very good. This is true in spite of the fact that the standing wave patterns at the downstream of the duct (where the anechoic boundary condition is imposed) are not captured. The comparison for the spanwise variable-impedance liners (SVC2 and SVC3) is less favorable than for the uniform (SVC1) liner, but still remains quite good.

Results achieved with the CDL code tend to overpredict the amount of absorption for all three liners at Mach 0.0 and 1000 Hz, although the difference in attenuation between the predicted results for the three liners is similar to that observed with the measured data. It should be noted that CDL assumes the input at the source plane is an incident wave, whereas the measured data consists of the incident and reflected waves. This difference in implementation is a basis for a portion of the difference between the measured and predicted levels, but is clearly not the dominant issue.

The comparison improves significantly for the other two frequencies (1050 and 1100 Hz) or Mach number (0.3). It is particularly interesting to note that a change in frequency of 50 Hz (from 1000 to 1050 Hz) causes the comparison of the CDL predictions and measured data to improve tremendously. A brief sensitivity study was conducted in an attempt to better understand this result. This study demonstrated that differences

American Institute of Aeronautics and Astronautics

between the CDL predictions and the measured data at frequencies near 1000 Hz could be virtually eliminated by varying the normalized resistance and/or reactance of the liner by ±0.05. This dramatic effect clearly demonstrates that very precise input data is required in this sensitive regime. Thus, a good portion of the difference between the acoustic pressures predicted by the CDL code and the measured data may be due to the accuracy of the KT method used for the initial impedance eduction process. When a similar variation of impedance (±0.05) was applied at a frequency well away from resonance (1600 Hz), the effect on the CDL predictions was virtually undetectable. Overall, the CDL code provides reasonable results unless the attenuation is quite large.
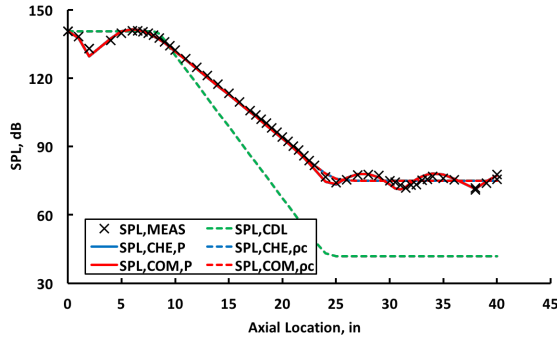
(a) SVC1 Liner, Mach 0.0.
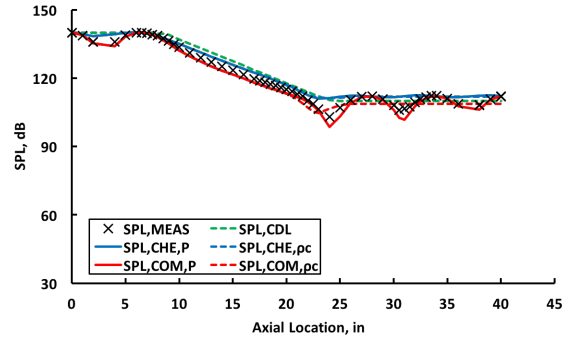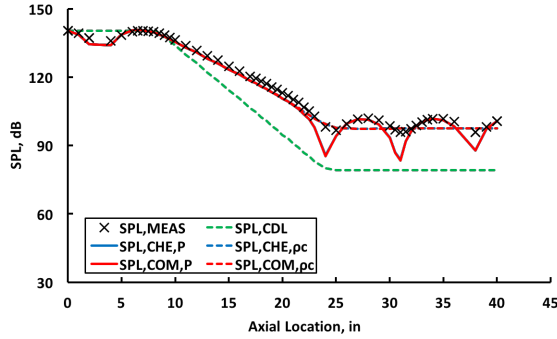
(b) SVC1 Liner, Mach 0.3.
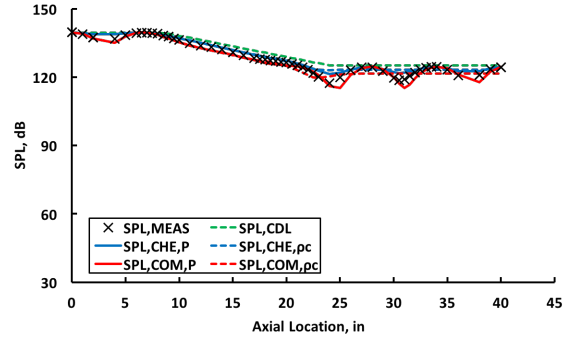
(c) SVC2 Liner, Mach 0.0.
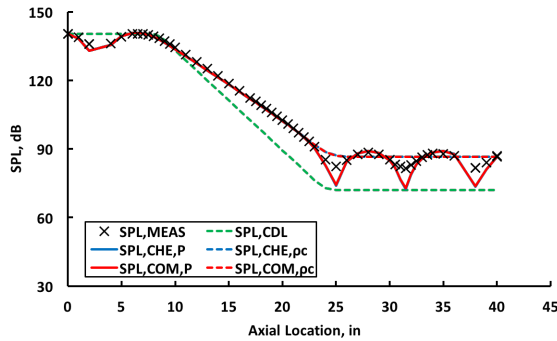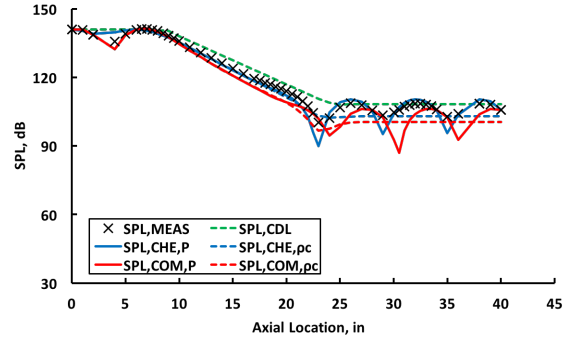
(d) SVC2 Liner, Mach 0.3.
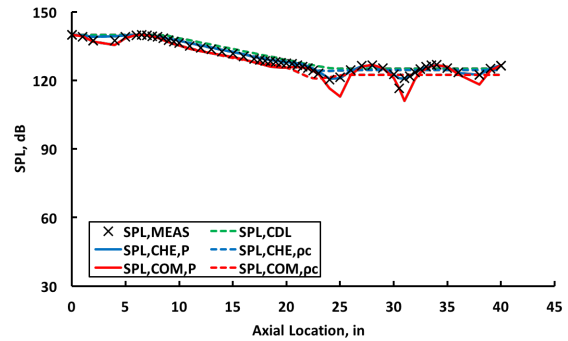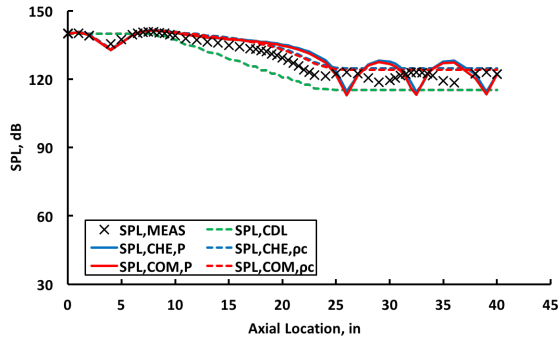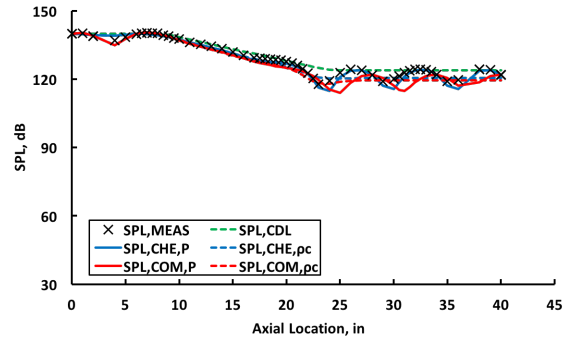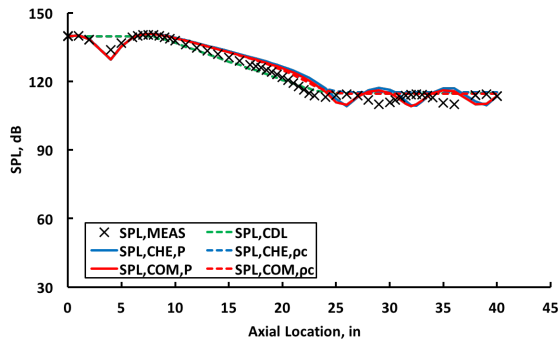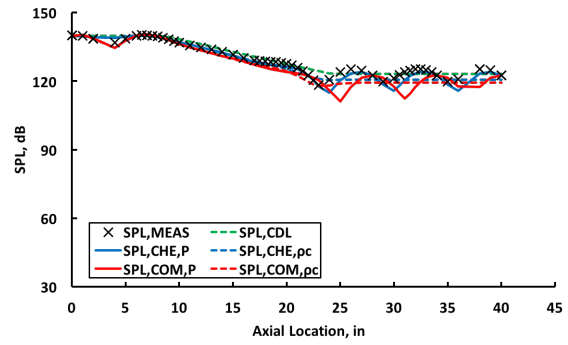
(e) SVC3 Liner, Mach 0.0.

(f) SVC3 Liner, Mach 0.3.

Figure 9: Comparison of predicted and measured SPL profiles. Frequency: 1000 Hz.
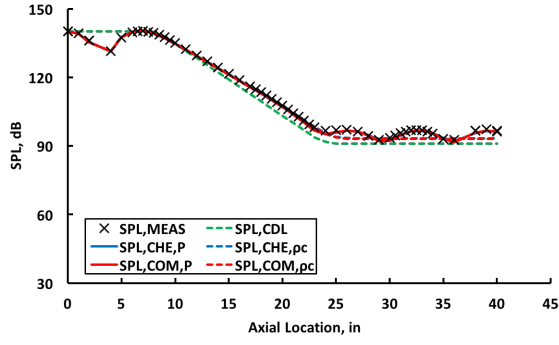
American Institute of Aeronautics and Astronautics

(a) SVC1 Liner, Mach 0.0.

(b) SVC1 Liner, Mach 0.3.

(c) SVC2 Liner, Mach 0.0.
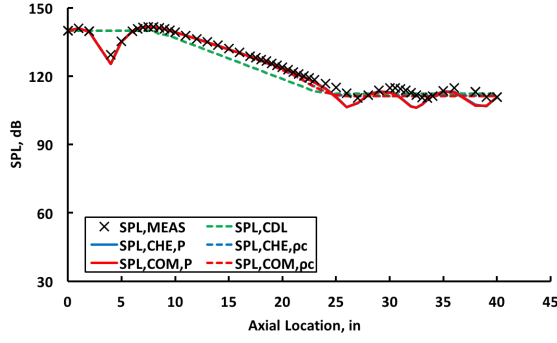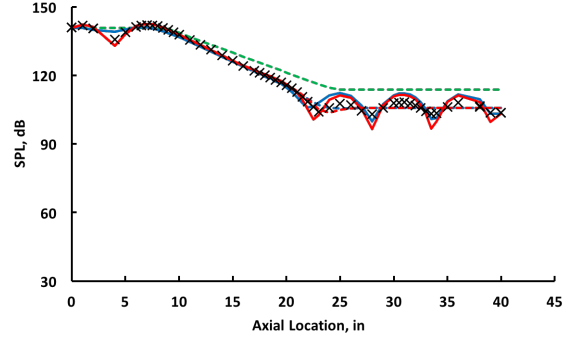
(d) SVC2 Liner, Mach 0.3.

(e) SVC3 Liner, Mach 0.0.

(f) SVC3 Liner, Mach 0.3.

Figure 10: Comparison of predicted and measured SPL profiles. Frequency: 1050 Hz.

American Institute of Aeronautics and Astronautics

(a) SVC1 Liner, Mach 0.0.

(b) SVC1 Liner, Mach 0.3.

(c) SVC2 Liner, Mach 0.0.

(d) SVC2 Liner, Mach 0.3.
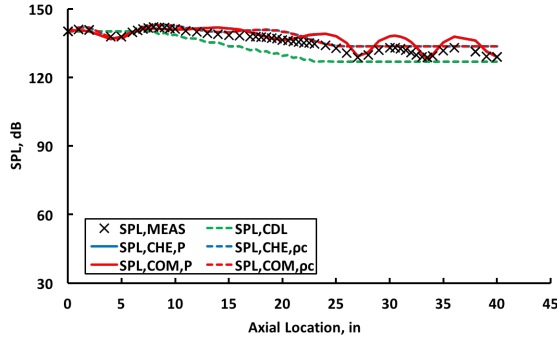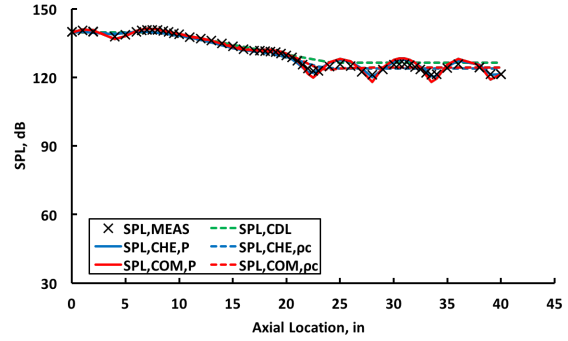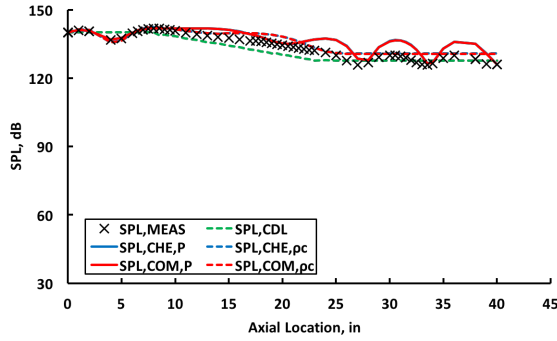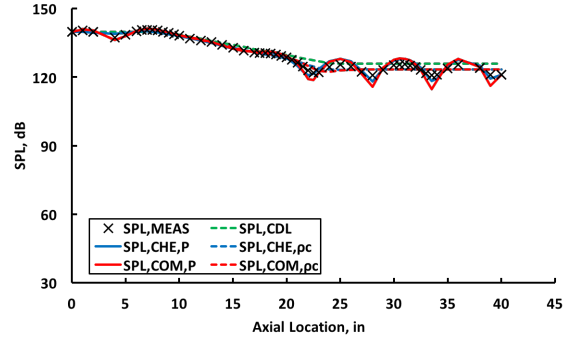
(e) SVC3 Liner, Mach 0.0.

(f) SVC3 Liner, Mach 0.3.

Figure 11: Comparison of predicted and measured SPL profiles. Frequency: 1100 Hz.

Figure 12 provides a comparison of the predicted and measured phase profiles for the uniform liner at Mach 0.0, at frequencies of 1000 and 1200 Hz. At 1000 Hz, the phase profile is noticeably flattened over much of the axial length of the liner (liner extends over $x \in \{8", 24"\}$). The corresponding phase profile at 1200 Hz, well away from resonance, is more 'conventional,' i.e., the phase decreases rather uniformly with increasing axial location. These comparisons between measured and predicted phase profiles are representative of the overall results. In general, the comparison is quite acceptable, although spurious deviations are not uncommon. Thus, the remainder of this paper concentrates on the SPL effects.
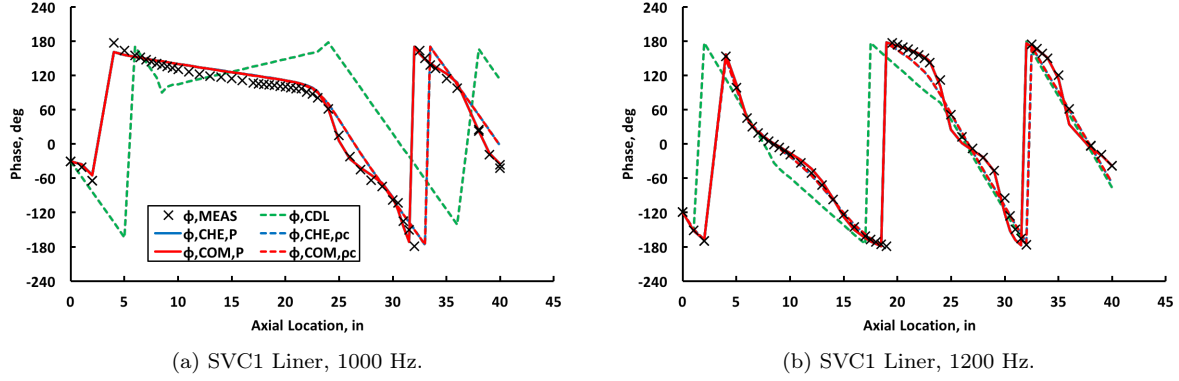
American Institute of Aeronautics and Astronautics

(a) SVC1 Liner, 1000 Hz.

(b) SVC1 Liner, 1200 Hz.

Figure 12: Comparison of predicted and measured phase (ϕ) profiles. Mach 0.0.

The results presented here represent a very small sampling of the full set of data. Thus, in an attempt to capture the 'goodness of fit' over the full range of test conditions, Figure 13 provides comparisons of the predicted and measured sound pressure levels for all 87 microphone locations (located on all four walls of the GFIT). The average error, $\bar{E}_{\mathrm{SPL}}$, is computed as

$$\bar{E}_{\mathrm{SPL}} = \frac{1}{n} \sum_{n=1}^{87} |\mathrm{SPL}_{\mathrm{meas}} - \mathrm{SPL}_{\mathrm{pred}}|_n \tag{1}$$

where $\mathrm{SPL}_{\mathrm{meas}}$ and $\mathrm{SPL}_{\mathrm{pred}}$ represent the measured and predicted sound pressure levels, respectively, and n represents the nth microphone location. For comparison, the data provided in the earlier figures (Figs. 4 - 7 and 9 - 11) presented the results for the microphone locations along the lower wall of the GFIT ($n \in \{23, 79\}$). Open symbols represent comparisons for the Mach 0.0 condition, and solid symbols represent the corresponding comparisons for the Mach 0.3 condition.

The average errors (average difference between measured and predicted SPL) for the two codes that employ an exit acoustic pressure condition (Figs. 13a and 13b) are very low for frequencies near resonance, and are slightly increased for frequencies away from resonance, where the attenuation is decreased. When the exit acoustic pressure condition is replaced with an anechoic termination (Figs. 13c and 13d), these two codes produce slightly larger error for frequencies near resonance but less error (relative to the two codes with an exit pressure condition) for frequencies away from resonance.

This latter observation is intriguing, as it would seem reasonable to expect that including more of the measured data (i.e., the exit plane acoustic pressure) in the prediction model would improve the comparisons with the full set of measured data. For those frequencies away from resonance, the reflections from the duct exhaust become a predominant feature in the SPL profiles due to the poor attenuation. The two codes with an exit pressure condition try to match this standing wave pattern, but have difficulty doing so. When the exit pressure condition is replaced by the anechoic termination, this duct exhaust reflection is ignored and the predictions tend to average out the measured standing waves. This results in a lower overall error, $\bar{E}_{\mathrm{SPL}}$.

Figure 13e provides the results for the CDL code. Similar to the results achieved with the CHE3D and COMSOL codes with an anechoic termination, the average error is smaller for those conditions where the attenuation is reduced (i.e., away from resonance for Mach 0.0, and across the full frequency range for Mach 0.3). When the attenuation is very large, the error is significantly increased. This is believed due, in large part, to the implementation of the parabolic approximation in the CDL code.

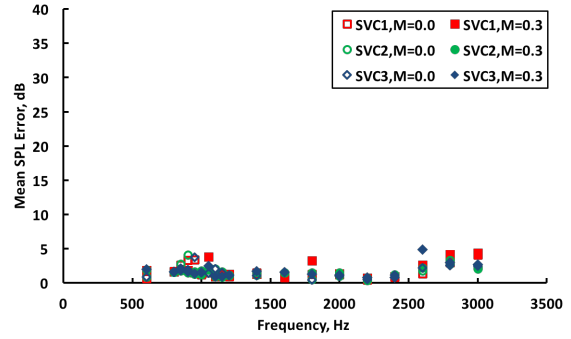American Institute of Aeronautics and Astronautics
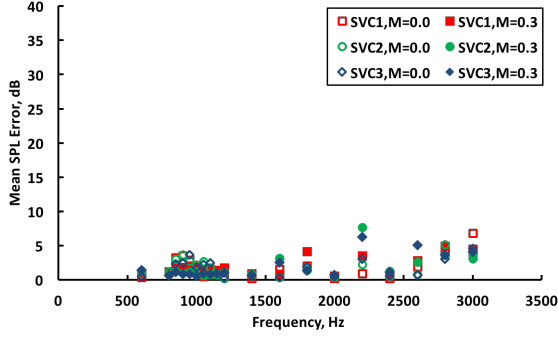
(a) Comparison of CHE3D predictions (pressure boundary condition; CHE,P) with measured data.
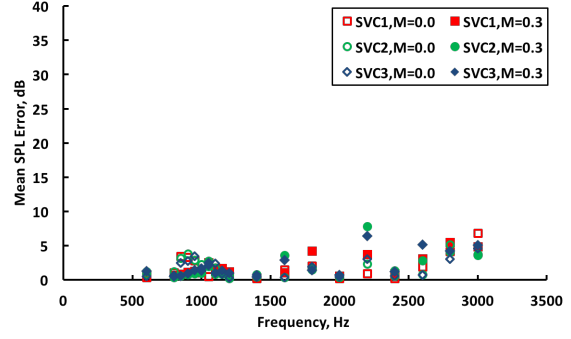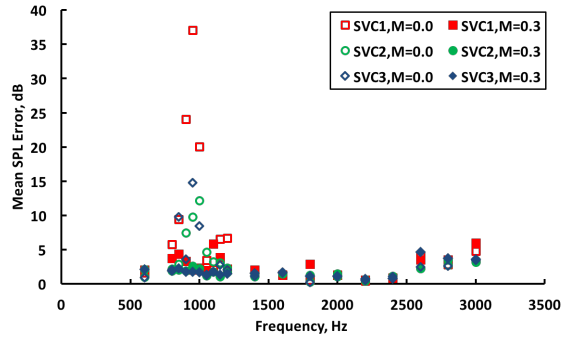
(b) Comparison of COMSOL predictions (pressure boundary condition; COM,P) with measured data.
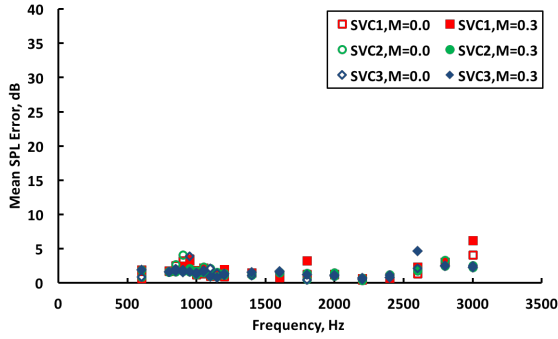
(c) Comparison of CHE3D predictions (ρc boundary condition; CHE,ρc) with measured data.

(d) Comparison of COMSOL predictions (ρc boundary condition; COM,ρc) with measured data.

(e) Comparison of CDL predictions with measured data.

Figure 13: Summary comparison of predicted and measured SPL differences.

VI. Concluding Remarks

The following conclusions are drawn from this study. First, although the GFIT is only 2" wide, impedance variability in the spanwise direction clearly affects the measured acoustic pressures along all four walls. Two spanwise variable-impedance liner configurations were used to demonstrate these effects. The impedance is distributed in an asymmetric manner for the first of these liner configurations, and in a symmetric manner for the other. This spanwise impedance variability is significant enough to require three-dimensional propagation codes to properly predict the acoustic pressure field.

Three 3D duct acoustic propagation codes (CHE3D, COMSOL, and CDL) were used to predict the

variable-impedance liner SPL and phase at each of the microphone locations in the GFIT (distributed along all four walls). The CHE3D and COMSOL codes (with an exit acoustic pressure boundary condition) compare favorably with the measured data for each of the three liner configurations and over a variety of test conditions. When the anechoic (ρc) termination is used, these codes continue to provide very reasonable estimates of the acoustic pressure distribution. Indeed, these favorable comparisons suggest that the common usage of the ρc termination condition for those cases where the measured data is unavailable is an acceptable approach. Finally, except for those frequencies where the attenuation is large, the CDL code also provides acceptable estimates of the measured acoustic pressure profile. The CHE3D and COMSOL predictions diverge slightly from the measured data for frequencies away from resonance, where the attenuation is noticeably reduced, particularly when an exit acoustic pressure boundary condition is used. For these conditions, the CDL predictions actually provide slightly more favorable comparison with the measured data.

Overall, the comparisons of predicted and measured data suggest that any of these codes can be used to understand data trends associated with spanwise variable-impedance liner configurations. However, it is noted that the aforementioned conclusions are only for plane-wave sources. Future studies are planned to explore the effects of higher-order mode sources.

Acknowledgments

References

[1] Parrott, T. L. and Jones, M. G., "Parallel-Element Liner Impedances for Improved Absorption of Broadband Sound in Ducts," *Noise Control Engineering Journal*, Vol. 43, No. 6, November - December, 1995.

[2] Jones, M. G., Howerton, B. M., and Ayle, E., "Evaluation of Parallel-Element, Variable-Impedance, Broadband Acoustic Liner Concepts," AIAA Paper 2012-2194, June 2012.

[3] Nark, D. M., Jones, M. G., , and Sutliff, D. L., "Further Development and Assessment of a Broadband Liner Optimization Process," AIAA Paper 2016-2784, May 2016.

[4] Jones, M. G., Watson, W. R., Nark, D. M., and Howerton, B. M., "Evaluation of a Variable-Impedance Ceramic Matrix Composite Acoustic Liner," AIAA Paper 2014-3352, June 2014.

[5] Kraft, R. E., "Theory and Measurement of Acoustic Wave Propagation in Multi-Sectioned Rectangular Ducts," Ph.d. dissertation, university of cincinnati, cincinnati, oh, May 1976.

[6] Sawdy, D. T., Beckemeyer, R. J., and Patterson, J. D., "Analytical and Experimental Studies of an Optimum Multisegment Phased Liner Noise Suppression Concept," NASA CR 134960, 1976.

[7] Lan, J. H., "Turbofan Duct Propagation Model," NASA CR 211245, 2001.

[8] Jones, M. G., Watson, W. R., Nark, D. M., Schiller, N. H., and Born, J. C., "Optimization of Variable-Depth Liner Configurations for Increased Broadband Noise Reduction," AIAA Paper 2016-2783, May 2016.

[9] Primus, J., Piot, E., Simon, F., Jones, M., and Watson, W., "ONERA-NASA cooperative effort on liner impedance eduction," AIAA Paper 2013-2273, May 2013.

[10] Watson, W. R. and Jones, M. G., "Impedance Eduction in 3D Sound Fields with Peripherally Varying Liners and Flow," AIAA Paper 2015-2228, June 2015.

[11] Nark, D. M. and Jones, M. G., "Broadband Liner Optimization for the Source Diagnostic Test Fan," AIAA Paper 2012-2195, June 2012.

[12] "COMSOL Acoustic Module User's Guide," v5.2a, 2016.

[13] Jones, M. G., Watson, W. R., and June, J. C., "Optimization of Microphone Locations for Acoustic Liner Impedance Eduction," AIAA Paper 2015-3271, June 2015.